EuroIntervention 2019;14:1685-1693 published online April 2018

Acute thrombogenicity of fluoropolymer-coated versus biodegradable and polymer-free stents

Sho Torii[1], MD, PhD; Qi Cheng[1], MD; Hiroyoshi Mori[1], MD; Michael J. Lipinski[2], MD, PhD; Eduardo Acampado[1], DVM; Laura E.L. Perkins[3], DVM, PhD; Syed F. Hossainy[3], PhD; Stephen D. Pacetti[3], MS; Frank D. Kolodgie[1], PhD; Renu Virmani[1], MD; Aloke V. Finn[1]*, MD

1. CVPath Institute, Inc., Gaithersburg, MD, USA; 2. Medstar Washington Hospital Center, Washington, DC, USA; 3. Abbott Vascular, Santa Clara, CA, USA

This paper also includes supplementary data published online at: http://www.pcronline.com/eurointervention/149th_issue/289

KEYWORDS

- ACS/NSTE-ACS
- bare metal stent
- drug-eluting stent
- preclinical research
- stable angina
- stent thrombosis

Abstract

Aims: Durable fluoropolymer-coated everolimus-eluting stents (FP-EES) have shown lower rates of stent thrombosis (ST) versus bare metal stents (BMS) and first-generation bioabsorbable polymer (BP) DES. The aim of the study was to evaluate the specific role of the FP in thromboresistance.

Methods and results: A total of 57 stents were assessed in three separate *ex vivo* swine arteriovenous shunt model experiments (first shunt experiment, custom-made fluoropolymer-coated BMS [FP-only] vs. BMS [n=8 each]; second shunt experiment, FP-EES vs. abluminally coated biodegradable polymer sirolimus-eluting stents [BP-SES] vs. BMS [n=8 each]; and third shunt experiment, FP-EES vs. polymer-free Biolimus A9-coated stents [PF-BCS] vs. BMS [n=6 each]). After one hour of circulation, stents were bisected, and each half was dual-immunostained using a platelet cocktail and a marker for inflammation. Antibody staining was visualised by confocal microscopy. In addition, stents were evaluated by scanning electron microscopy. FP-only stents showed significantly lower platelet adherence compared with BMS (% fluorescence-positive area: FP-only=1.8%, BMS=5.6%, p=0.047) with similar inflammatory cell density. FP-EES also demonstrated the lowest platelet adherence compared with BP-SES (p=0.056), PF-BCS (p=0.013) and BMS (p=0.003) with the significantly lowest inflammatory cell density.

Conclusions: Fluoropolymer coating imparts greater thromboresistance relative to BMS and to polymer-free DES designs, which reflects an unique phenomenon known as fluoropassivation, representing one proposed mechanism for clinically observed low ST rates in FP-EES.

**Corresponding author: CVPath Institute, Inc., 19 Firstfield Road, Gaithersburg, MD 20878, USA.*
E-mail: AFinn@CVPath.org

SUBMITTED ON 14/08/2017 - REVISION RECEIVED ON 1st 06/12/2017 / 2nd 15/02/2018 / 3rd 27/02/2018 - ACCEPTED ON 29/03/2018

DOI: 10.4244/EIJ-D-17-00728

Abbreviations

BMS bare metal stents
BP-SES biodegradable polymer sirolimus-eluting stents
FP-EES fluoropolymer-coated everolimus-eluting stents
FP-only fluoropolymer-coated stents
PF-BCS polymer-free Biolimus A9-coated stents
ST stent thrombosis

Introduction

Recent comprehensive meta-analyses of clinical trials established that durable fluoropolymer (poly[vinylidene fluoride-co-hexafluoropropylene] [PVDF-HFP])-coated everolimus-eluting stents (FP-EES) have lower rates of stent thrombosis (ST) and target vessel revascularisation than bare metal stents (BMS) or thick-strut biodegradable polymer drug-eluting stents (BP-DES)[1,2]. A previous preclinical arteriovenous swine shunt study demonstrated superior acute thromboresistance for FP-EES relative to BMS and BP-DES[3,4], which supports the prior clinical observations regarding lower ST for FP-EES. However, it still remains uncertain whether other components of FP-EES besides the polymer itself might be responsible for these findings. Moreover, stent designs have continued to evolve with many newer stent designs having thinner struts, while some do not contain polymers. These design differences raise the question of whether FP-EES still hold a thromboresistance advantage versus newer stent designs.

More recently developed BP-DES have demonstrated non-inferiority to FP-EES for the composite primary endpoint of safety and efficacy in several randomised controlled trials[5,6]. Polymer-free Biolimus A9-coated stents (PF-BCS), another new concept in DES design, have demonstrated superior clinical outcomes compared to early paclitaxel-eluting stents[7]. The common concept of most newer DES is based on the idea that polymers are "harmful". The idea has been raised from the unfavourable clinical results of the first-generation DES due to the durable polymers that have been associated with inflammatory responses and hypersensitivity reactions[8-10].

Here we specifically tested the hypothesis that the FP on EES is the most important component of its design with respect to thromboresistance by comparing stents of similar design with and without FP coating (i.e., no drug) in a swine *ex vivo* shunt model. The acute thrombogenicity of FP-EES was also compared with thin-strut abluminally coated BP-DES and PF-DES to examine whether FP-EES still hold an advantage with respect to acute thrombogenicity versus these newer stent designs.

Methods

SWINE EX VIVO ARTERIOVENOUS SHUNT MODEL

The study protocol was reviewed and approved by the Institutional Animal Care and Use Committee and met the ARRIVE guidelines. For each procedure, pigs were anaesthetised with ketamine/xylazine, intubated and maintained under general anaesthesia with isofluorane. A swine *ex vivo* carotid to jugular arteriovenous shunt model was established to study the extent of platelet adherence, thrombus formation, and acute inflammation, as previously described[3,11] **(Supplementary Appendix 1)**. Three separate shunt studies were performed. In the first shunt study, custom-made fluoropolymer-only coated MULTI-LINK 8™ BMS (Abbott Vascular, Santa Clara, CA, USA) without everolimus (FP-only [n=8]) and MULTI-LINK 8 BMS (no polymer [n=7]) were compared. In the second shunt study, XIENCE Alpine™ EES (Abbott Vascular) with durable fluoropolymer (FP-EES [n=8]), Ultimaster® (Terumo Corp., Tokyo, Japan) abluminally coated biodegradable polymer sirolimus-eluting stents (BP-SES [n=8]), and MULTI-LINK VISION® (Abbott Vascular) BMS (n=8) were compared. In the third shunt study, FP-EES (n=6), the polymer-free Biolimus A9™-coated stent (BioFreedom™; Biosensors International, Singapore) (PF-BCS [n=6]), and the MULTI-LINK VISION BMS (n=6) were compared **(Supplementary Figure 1)**. In summary, a total of 57 stents were deployed in 19 shunts from 10 swine for the assessment of acute thrombogenicity.

The extent of platelet aggregation to struts was studied after exposure to circulating blood for one hour through an established arteriovenous carotid to jugular shunt. Blood activated clotting times (ACT) were measured every 20 minutes and targeted to be between 150 s and 190 s using intravenous heparin (100 IU/kg) without antiplatelet agents.

ASSESSMENT OF PLATELET AGGREGATION AND INFLAMMATION

CONFOCAL MICROSCOPY

Stent halves were incubated overnight in an antibody cocktail directed against specific platelet markers – a platelet cocktail of CD61 and CD42b. Each half was processed for immunostaining using an inflammatory marker for neutrophils (PM-1) or monocytes (CD14). The positive area of platelet staining was analysed by proprietary software within the entire bisected segment of the stented artery, which was maintained for all examined samples and reported as absolute positive area (mm^2) of the device and percentage of positive area.

SCANNING ELECTRON MICROSCOPY (SEM)

After confocal microscopy, stent halves were processed for SEM. Low-power images of the entire luminal surface were collected to assess the extent of thrombus attached to the strut surfaces. The percentage of thrombus coverage was estimated visually for each row of struts corresponding to a ring.

QUANTIFICATION OF INFLAMMATORY CELLS

Images for quantification of inflammatory cells were acquired at every other strut in regions relatively free of platelet thrombus. The number of inflammatory cells was manually counted and expressed as cell density (cells/mm^2) relative to the strut surface area.

STATISTICAL ANALYSIS

Nested generalised linear mixed models (GLMM) with Dunnett's correction for multiple testing were employed in order to investigate group differences in consideration of multiple measurements per individual. Within these models, stent type was considered as fixed effect, while the experimental factor variables animal, shunt number and linear position were considered as nested random effects.

Values are expressed as estimated mean with 95% confidence interval (CI). To assess the consistency of the three shunt experiments, thrombus-occupied area and inflammatory cell density of BMS in three shunt experiments were also compared using GLMM with Dunnett's correction for multiple testing. The analyses were performed with SPSS Advanced Statistics, Version 22 (IBM Corp., Armonk, NY, USA). The statistical tests were two-tailed and a value of $p<0.05$ was considered to indicate statistical significance[12].

Results

BLOOD COAGULATION AND PLATELET FUNCTION

There was no evidence of blood coagulation or platelet function abnormalities in any of the animals studied. The mean ACT was 174.7±17.2 seconds during the first shunt and 167.2±17.6 seconds during the second shunt for the 10 swine included in this study **(Supplementary Table 1, Supplementary Table 2)**.

SHUNT EXPERIMENT 1 (FP-ONLY VS. BMS)

FP-only stents demonstrated percent positive fluorescence areas for CD42b/CD61 corresponding to aggregated platelets which were less compared with BMS (FP-only=1.8%, BMS=15.6%, p=0.047) **(Figure 1, Figure 2, Table 1)**. Percent thrombus areas assessed by SEM were also significantly less in FP-only compared with BMS (FP-only=2.4%, BMS=21.3%, p=0.019) **(Figure 2, Figure 3)**.

On the other hand, cell density of monoytes (CD14) and neutrophils (PM-1) on strut surfaces was similar in FP-only and BMS (monocytes [CD14]: FP-only=198.0 cells/mm^2 vs. BMS=209.7 cells/mm^2, p=0.712; neutrophils [PM-1]: FP-only=288.1 cells/mm^2 vs. BMS=381.8 cells/mm^2, p=0.161) **(Figure 4, Figure 5)**.

SHUNT EXPERIMENT 2 (FP-EES VS. BP-SES VS. BMS)

FP-EES demonstrated the least percent positive fluorescence areas for CD42b/CD61 compared with BP-SES and BMS (FP-EES=4.1%, BP-SES=7.6%, BMS=25.1%) **(Figure 1, Figure 2, Table 1)**; however, the difference between FP-EES and BP-SES did not reach statistical significance by linear mixed-effects model (p=0.056), whereas the difference between FP-EES and BMS reached statistical significance (p=0.003) **(Figure 2)**. Percent thrombus areas assessed by SEM also demonstrated similar results as shown in confocal assessment **(Figure 2, Figure 3)**.

Cell density of monocytes (CD14) and neutrophils (PM-1) on strut surfaces was significantly less in FP-EES compared with BP-SES (monocytes [CD14]: FP-EES=46.3 cells/mm^2 vs. BP-SES=159.0 cells/mm^2, p=0.001; neutrophils [PM-1]: FP-EES=72.3 cells/mm^2 vs. BP-SES=230.6 cells/mm^2, p=0.001) and BMS (monocytes [CD14]: BMS=293.6 cells/mm^2, p<0.001; neutrophils [PM-1]: 379.2 cells/mm^2, p=0.004) **(Figure 4, Figure 5)**.

SHUNT EXPERIMENT 3 (FP-EES VS. PF-BCS VS. BMS)

PF-BCS demonstrated the highest percent positive fluorescence areas for CD42b/CD61 compared with FP-EES (PF-BCS=46.5%, FP-EES=2.2%, BMS=25.9%) **(Figure 1, Figure 2, Table 1)**. The linear mixed-effects model demonstrated statistical significance between PF-BCS and FP-EES (p=0.013), and BMS and FP-EES (p=0.016), whereas the difference of PF-BCS and BMS did not reach statistical significance (p=0.195) **(Figure 2)**. Percent thrombus areas assessed by SEM also demonstrated similar results as shown in confocal assessment **(Figure 2, Figure 3)**.

Table 1. Estimated means with 95% confidence interval of percent fluorescence positive area by confocal microscopy (CM), platelet thrombus area by scanning electron microscopy (SEM), number of CD14 (monocytes) positive cells by CM, and number of PM-1 (neutrophils) positive cells by CM in a swine acute shunt model.

Shunt experiment 1	FP only	BMS		*p*-values		
				FP only vs. BMS		
CD42b/CD61 positive area, % by CM	1.8 (0.7-5.0)	15.6 (5.9- 41.6)		0.047		
CD42b/CD61 positive area, % by SEM	2.4 (1.1-5.1)	21.3 (9.8-46.0)		0.019		
CD14 positive cells, cell number/mm^2	198.0 (156.8-250.1)	209.7 (163.6-268.8)		0.712		
PM-1 positive cells, cell number/mm^2	288.1 (218.0-380.7)	381.8 (283.5-514.2)		0.161		
Shunt experiment 2	**FP-EES**	**BP-SES**	**BMS**	**FP-EES vs. BP-SES**	**FP-EES vs. BMS**	**BP-SES vs. BMS**
CD42b/CD61 positive area, % by CM	4.1 (2.4-7.2)	7.6 (4.4-13.4)	25.1 (14.3-43.9)	0.056	0.003	0.008
CD42b/CD61 positive area, % by SEM	4.8 (2.9-7.9)	8.2 (4.9-13.6)	33.1 (19.9-54.9)	0.091	0.002	0.004
CD14 positive cells, cell number/mm^2	46.3 (30.7-69.9)	159.0 (105.5-239.6)	293.6 (194.8-422.6)	0.001	<0.0001	0.018
PM-1 positive cells, cell number/mm^2	72.3 (49.3-105.9)	230.6 (157.3-338.0)	379.2 (258.7-555.8)	0.001	<0.0001	0.224
Shunt experiment 3	**FP-EES**	**PF-BCS**	**BMS**	**FP-EES vs. PF-BCS**	**FP-EES vs. BMS**	**PF-BCS vs. BMS**
CD42b/CD61 positive area, % by CM	2.2 (1.1-4.6)	46.5 (22.3-97.0)	25.9 (12.4-54.0)	0.013	0.016	0.195
CD42b/CD61 positive area, % by SEM	3.6 (1.9-6.6)	53.0 (28.4-96.9)	27.1 (14.5-50.7)	0.005	0.008	0.099
CD14 positive cells, cell number/mm^2	53.7 (26.0-111.1)	421.9 (204.1-872.4)	298.1 (144.2-616.3)	0.013	0.015	0.224
PM-1 positive cells, cell number/mm^2	46.3 (25.8-83.0)	1,172.0 (652.8-2,104.3)	530.3 (295.3-952.1)	0.003	0.004	0.063

Values are expressed as estimated mean with 95% confidence interval.

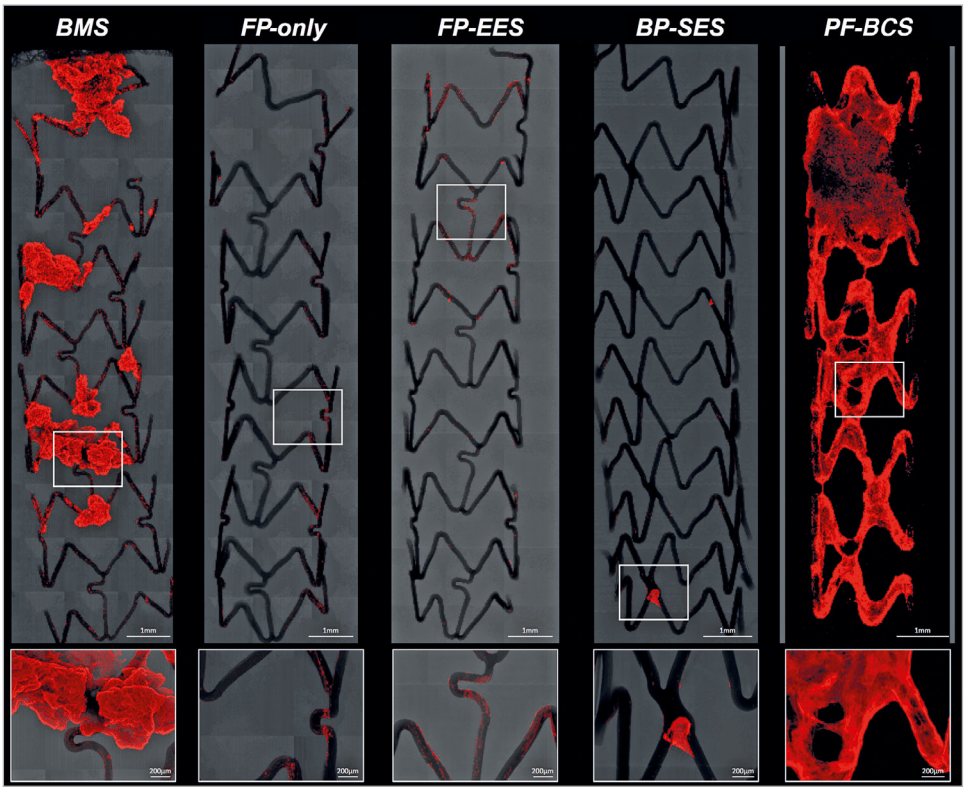

Figure 1. *Representative confocal microscopic images of BMS, FP-only, FP-EES, BP-SES, and PF-BCS with immunofluorescent staining against dual platelet markers (CD61/CD42b) in a swine shunt model. Low- and high-power confocal microscopic images showing the least thrombus-occupied area in stents with fluoropolymer (FP-only and FP-EES) as compared with the other stents. Note minimal thrombus is only observed in the link portion of FP-only and FP-EES, whereas large thrombus covers almost all the struts in PF-BES.*

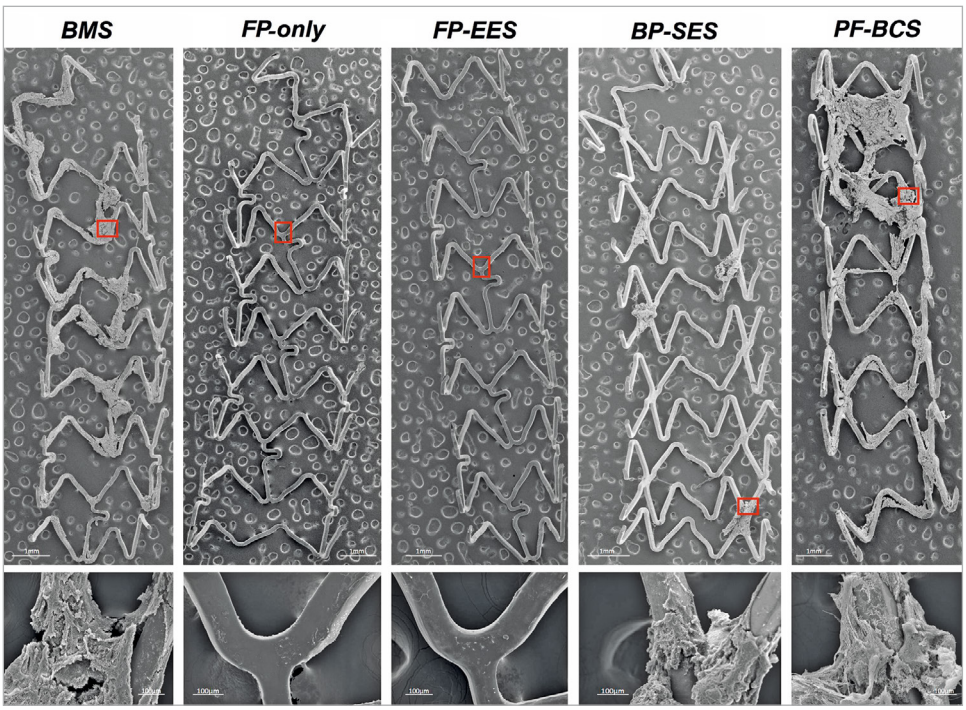

Figure 2. *Representative scanning electron microscopic images of BMS, FP-only, FP-EES, BP-SES, and PF-BCS in a swine shunt model. Low- (×15) and high- (×200) power images of scanning electron microscopy showing least platelet aggregation clot formation (red boxes) on stents with fluoropolymer (FP-only and FP-EES) as compared with the other stents.*

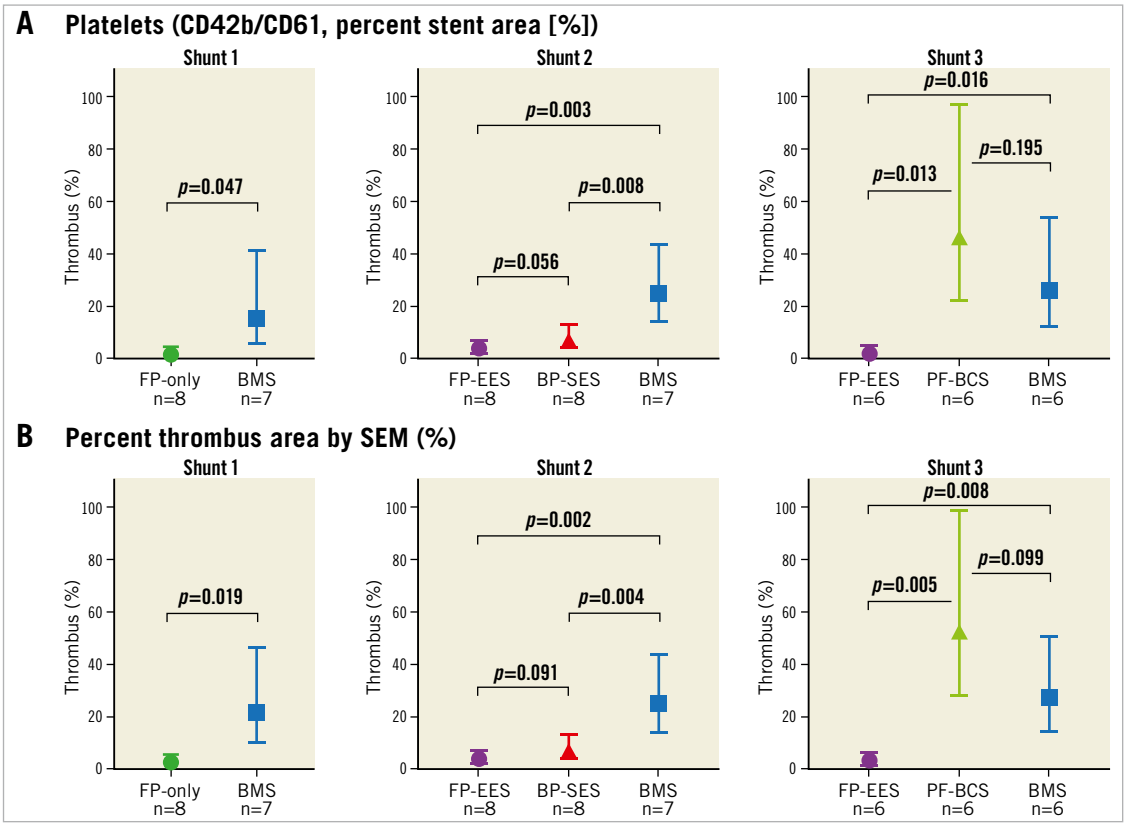

Figure 3. *Comparisons of acute thrombogenicity on the stent surface in a swine shunt model. Graph with 95% confidence interval showing percent fluorescent positive area (percent area occupied by thrombus) assessed by confocal microscopy (A) and SEM (B) from three shunt models (first shunt experiment, FP-only vs. BMS; second shunt experiment, FP-EES vs. BP-SES vs. BMS; and third shunt experiment, FP-EES vs. PF-BCS vs. BMS).*

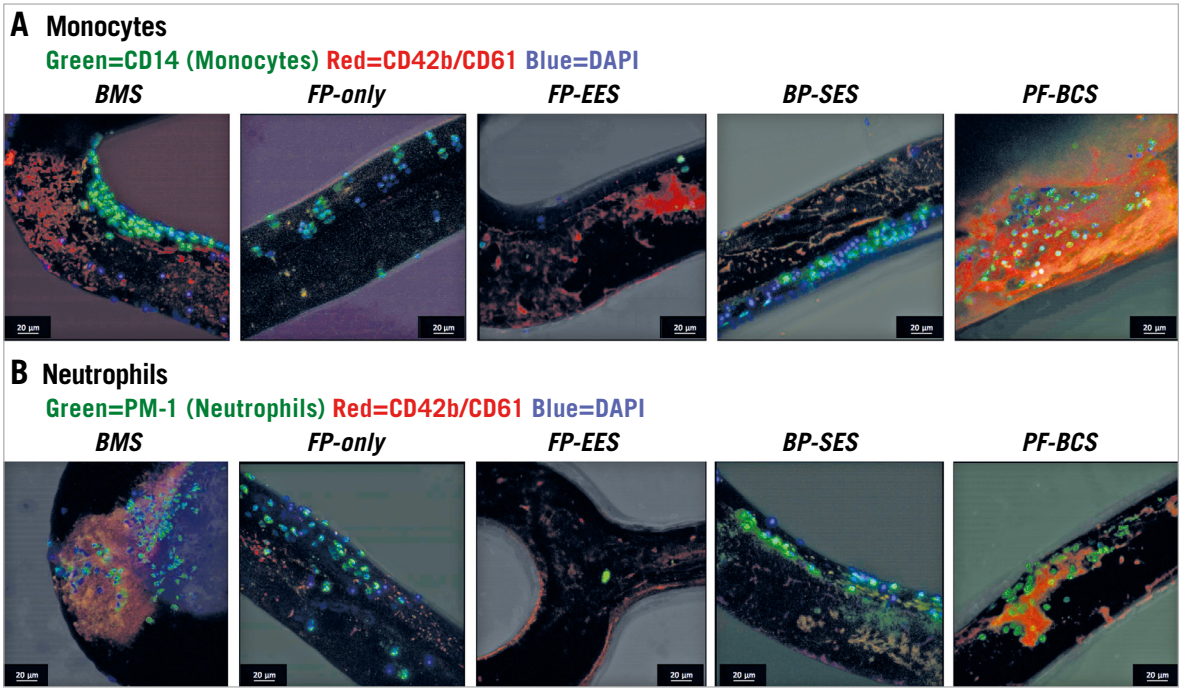

Figure 4. *Representative confocal images of each stent with inflammatory cells in a swine shunt model. CD14 stained nuclei represent adherent monocytes (A), whereas PM-1 stained nuclei represent adherent neutrophils (B).*

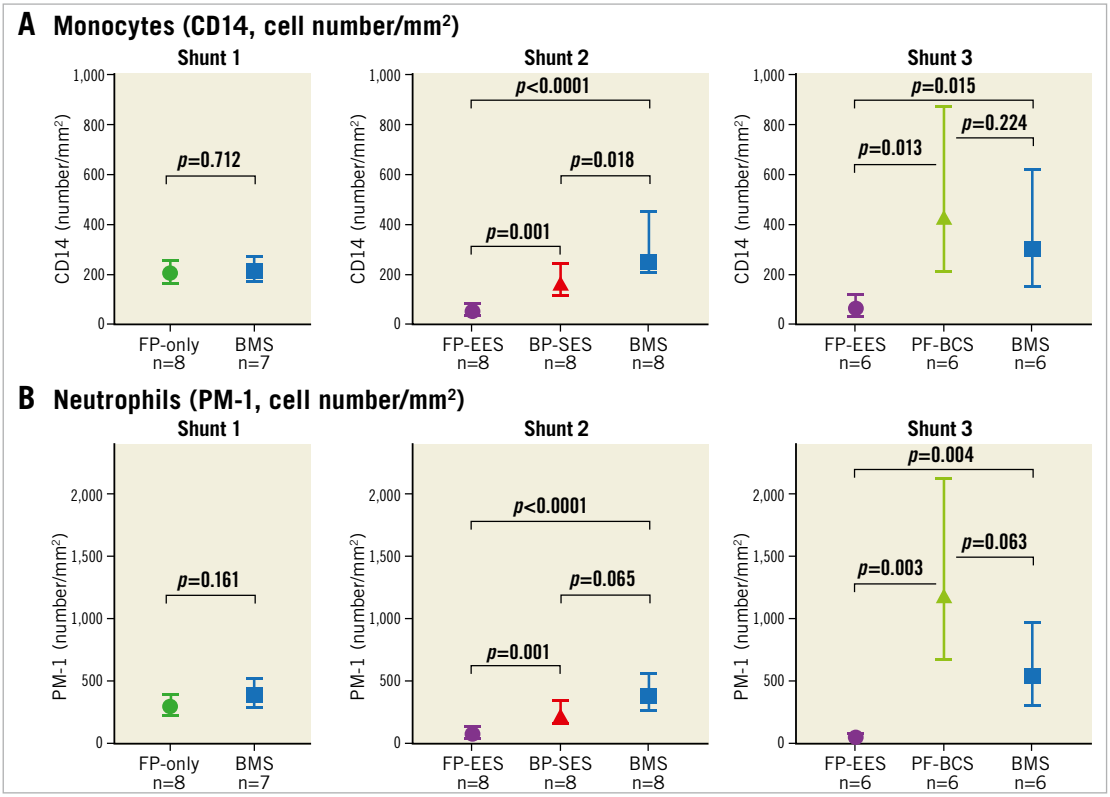

Figure 5. *Comparisons of inflammatory cell attachment on the stent surface in a swine shunt model. Graph with 95% confidence interval showing number of monocytes (CD14) (A) and neutrophils (PM-1) (B) assessed by confocal microscopy from three shunt models (first shunt experiment, FP-only vs. BMS; second shunt experiment, FP-EES vs. BP-SES vs. BMS; and third shunt experiment, FP-EES vs. PF-BCS vs. BMS).*

Cell density of monocytes (CD14) and neutrophils (PM-1) on strut surfaces was significantly higher in PF-BCS compared with FP-EES (monocytes [CD14]: PF-BCS=421.9 cells/mm² vs. FP-EES=53.7 cells/mm², p=0.013; neutrophils [PM-1]: PF-BCS=1,172.0 cells/mm² vs. FP-EES=46.3 cells/mm², p=0.003). There was no difference in either inflammatory cell type between PF-BCS compared with BMS (monocytes [CD14]: BMS=298.1 cells/mm², p=0.22; neutrophils [PM-1]: BMS=530.3 cells/mm², p=0.063) **(Figure 4, Figure 5)**.

PLATELET AGGREGATION AND INFLAMMATORY CELL ADHESION OF BMS IN THREE SHUNT EXPERIMENTS

There were no significant differences among the three BMS used in the three shunt experiments, respectively, in positive fluorescence areas for CD42b/CD61, percent thrombus areas, and cell density of both monocytes and neutrophils **(Supplementary Table 3)**.

Discussion

FP-EES have been associated with a lower risk of ST when compared to BMS and early thick-strut BP-DES, but which component of the stent is responsible for this lower ST risk as well as its performance relative to contemporary DES remains uncertain. The current study examined acute thrombogenicity with respect to platelet aggregation and inflammatory cell adhesion of various stents including custom fluoropolymer-only stents without everolimus using an established *ex vivo* swine arteriovenous shunt model. The principal findings in the current preclinical study are as follows. 1) Custom fluoropolymer-only XIENCE stents without everolimus demonstrated a significantly lower percentage of thrombus-occupied area than BMS (p=0.047) with similar inflammatory cell density. 2) FP-EES demonstrated the least percentage of thrombus-occupied area compared with BP-SES (p=0.056), PF-BCS (p=0.013) and BMS (shunt experiment 2, p=0.003; shunt experiment 3, p=0.016) with the lowest inflammatory cell density. 3) BMS demonstrated similar thrombus-occupied area and inflammatory cell density in all three shunt experiments, suggesting consistency among the shunt runs.

ROLE OF FLUOROPOLYMER

This study is the first study to have evaluated the thromboresistance of the FP-coated stent itself using custom FP-only stents without everolimus and matched BMS in an acute *ex vivo* shunt model. The fluoropolymer coating alone imparts greater thromboresistance as compared to a BMS with the same stent platform.

Fluoropolymers have known ability to reduce platelet adhesion and activation compared to controls. Platelet adhesion and activation were more strongly suppressed as the amount of fluorine dosing was increased[13,14]. A recent *in vitro* study performed by our group demonstrated a significantly higher antithrombogenic effect of the fluoropolymer compared with the various polymers used in the

early durable polymer DES[13]. Fluoropassivation is a blood contact phenomenon by which fluorinated surfaces elicit a decreased local thrombotic response[15-18]. Unlike hydrophobic polymers that showed thromboresistance in an *in vivo* rabbit model[19], fluoropassivation is thought to result from preferential affinity for albumin and retention of albumin. This albumin-rich protein layer modulates host-material interface interactions and competitively inhibits the adhesion of prothrombotic proteins, such as fibrinogen[13,20]. This mechanism of albumin retention and spreading depends on surface hydrophobicity[21]. PVDF-HPF surface coating on CoCr-EES/Pt-Cr-EES has a carbon backbone of which more than 50% is saturated with fluorine to form a hydrophobic surface. The protein spreading rate increases with substrate hydrophobicity ranging from 0.02 to 0.16 nm^2/molecule/s for albumin[21]: fluoropolymers possess an extremely high degree of hydrophobicity (for example, PVDF homopolymer has an equilibrium water adsorption in a range from 0.01% [w/w] to <0.04% [w/w]). Additionally, high bond strength, low polarisability and a high degree of fluorination also contribute to fluoropolymer interaction with culprit proteins such as fibrinogen and vWF.

On the other hand, anti-inflammatory effects were similar between FP-only stents and BMS, whereas fluoropolymer-coated everolimus-eluting stents with the same stent platform (FP-EES) demonstrated significantly lower inflammatory cell adhesion compared with BMS. The result suggests that there are two mechanisms of superior clinical outcomes of FP-EES: thromboresistance owing to the fluoropolymer, with an additional local anti-inflammatory effect owing to the drug (everolimus) release from a circumferential coating that covers all strut surfaces. Further studies are needed to reveal the difference between fluoropolymer and other durable polymers of contemporary DES (e.g., BioLinx polymer [a mixture of C10/C19, and polyvinylpyrrolidine polymers] in the Resolute Onyx™ zotarolimus-eluting stent [Medtronic, Minneapolis, MN, USA][22,23]). Although not specifically examined here, we have also shown recently in human autopsy cases minimal inflammatory reaction surrounding stents coated with fluoropolymer surfaces (i.e., CoCr-EES) versus bare metal surfaces implanted for greater than one year[24]. Thus the debate about whether polymer exposure should be minimised depends upon the type of polymer used.

DIFFERENCE BETWEEN CIRCUMFERENTIALLY COATED DURABLE FLUOROPOLYMER AND ABLUMINALLY COATED BIODEGRADABLE POLYMER

The BP-SES (Ultimaster) used in the current study is abluminally coated with a biodegradable polymer in which the luminal surface of the stent remains a bare metal surface. One of the proposed goals of abluminally coated polymer is to induce faster endothelial coverage[23]. However, abluminally coated BP-SES showed numerically greater platelet aggregation (p=0.056) compared with FP-EES, and the result is consistent with our previous preclinical study[3] that demonstrated significantly greater platelet aggregation in the CE-marked abluminally coated BP-DES (SYNERGY™; Boston Scientific, Marlborough, MA, USA). These results suggest that the "bare metal" surface might be one of the causes of acute thrombogenicity, and thrombus could aggregate on the bare surface of the luminal side in the abluminally coated BP-DES. Kolandaivelu et al also measured greater thrombogenicity for BMS compared to polymer-coated DES in an *in vitro* model[4]. On the other hand, BP-SES showed superior thromboresistance (p=0.008) compared with BMS. As both BP-SES and BMS have bare metal luminal surfaces, this difference may be due to the presence of the drug. Some data suggest that BP-DES that are coated only abluminally lack coating integrity upon deployment and also during acute time points (zero to two months)[25,26]. The FP-EES coating integrity and fluoropassivation phenomena may combine to contribute to its greater thromboresistance relative to BP-DES. The significantly lower inflammatory cell adhesion of FP-EES compared with BP-SES may be attributed to the elution of everolimus from the luminal and strut sidewall surfaces.

CIRCUMFERENTIALLY COATED FP-EES VS. POLYMER-FREE BCS

PF-BCS (BioFreedom) demonstrated higher platelet adherence compared with FP-EES. We assume that the reason for the higher acute thrombogenicity of PF-BCS could be that the abluminal surface of the PF-BCS is selectively microstructured which allows adhesion of the antiproliferative agent (Biolimus A9) to the abluminal surface of the stent without a polymer or binder[27]. Although the rough microstructured surface may contribute to faster endothelialisation[27], it also increases platelet adherence compared with smooth fluoropolymer or metallic surface in the very acute phase.

Biolimus A9 is coated on the abluminal surface of PF-BCS; however, the anti-inflammatory effect of PF-BCS was significantly less than FP-EES, and was similar to that of BMS. Not only is it the bare metal surface of the luminal side that causes inflammatory cell adherence as previously described, but also aggregated thrombus might be a reason for the current result because platelet aggregation on the surface of stent struts is known to be a trigger to recruit circulating leukocytes consisting mainly of neutrophils and monocytes[28].

CLINICAL IMPLICATIONS

In the first-generation DES era, durable polymers employed in these devices were associated with ST, in part due to inflammation and hypersensitivity reactions[9]. Clinical trials also demonstrated a higher incidence of ST compared with BMS. These results suggested untoward effects of durable polymers and helped to spur the development of biodegradable polymer DES and polymer-free DES that leave a bare metal surface behind in a few months after the stent implantation. On the other hand, the durable fluoropolymer DES have demonstrated lower ST rates in several clinical trials and meta-analyses, and the result is consistent with the current preclinical study. Our study suggests important antithrombotic benefits of FP-EES which continue to compare favourably versus other stents.

Limitations

There are some limitations in the current study. First, this study was performed with a swine *ex vivo* shunt model without antiplatelet agents, so that applying preclinical findings to human diseased

coronary arteries with dual antiplatelet therapy is more complex. Although this model is relatively simplistic in order to allow direct cross comparison of stents between shunts, this simple model cannot account for all the potential variables than can contribute to acute thrombogenicity in diseased human coronary arteries. Second, although systemic effects of the coated drug in DES are low and transient, becoming undetectable quickly, the drug eluted from a DES may affect inflammatory cell adhesion of the adjacent stent in this model. However, we believe that the established *ex vivo* shunt model in the current study could account for a number of covariates influencing acute platelet aggregation, thrombus formation, and leukocyte adhesion, and would be more likely to resemble flow conditions which occur in humans *in vivo* compared with an *in vitro* flow loop model.

Conclusions

Our data suggest that the choice of surface covering of metallic stents is an important determinant of the relative thromboresistance profile of different DES. Fluoropolymer coating imparts greater thromboresistance relative to BMS and to polymer-free DES designs, which reflects an unique phenomenon known as fluoropassivation, representing one proposed mechanism for clinically observed low ST rates in FP-EES.

Impact on daily practice

In this study, fluoropolymer-only stents showed significantly lower platelet adherence compared with BMS with similar inflammatory cell density. FP-EES also demonstrated the lowest platelet adherence compared with BP-SES, PF-BCS and BMS with the lowest inflammatory cell density. The results reflect an unique phenomenon known as fluoropassivation, representing an important mechanism for clinically observed low stent thrombosis rates in FP-EES.

Acknowledgements

We are grateful to Dr Fuh-Wei Tang and Darry Valdemoro of Abbott Vascular for their work on fabrication of the fluoropolymer-only coated stents.

Funding

This study was funded by Abbott Vascular, Santa Clara, CA, USA. CVPath Institute, Inc., Gaithersburg, MD, USA provided full support for this work.

Conflict of interest statement

S. Torii receives honoraria from Abbott Vascular Japan and Terumo Corporation, and research grants from SUNRISE lab. R. Virmani and A. Finn have received institutional research support from Abbott Vascular, Biosensors International, Biotronik, Boston Scientific, Medtronic, MicroPort Medical, OrbusNeich Medical, SINO Medical Technology, and Terumo Corporation. R. Virmani has speaking engagements with Merck, receives honoraria from Abbott Vascular, Boston Scientific, Lutonix, Medtronic, and Terumo Corporation, and is a consultant for 480 Biomedical, Abbott Vascular, Medtronic, and W.L. Gore. L. Perkins, S. Hossainy, and S. Pacetti are full-time employees of Abbott Vascular. The other authors have no conflicts of interest to declare.

References

1. Sakurai R, Burazor I, Bonneau HN, Kaneda H. Long-term outcomes of biodegradable polymer biolimus-eluting stents versus durable polymer everolimus-eluting stents: A meta-analysis of randomized controlled trials. *Int J Cardiol.* 2016;223:1066-71.

2. Palmerini T, Biondi-Zoccai G, Della Riva D, Stettler C, Sangiorgi D, D'Ascenzo F, Kimura T, Briguori C, Sabate M, Kim HS, De Waha A, Kedhi E, Smits PC, Kaiser C, Sardella G, Marullo A, Kirtane AJ, Leon MB, Stone GW. Stent thrombosis with drug-eluting and bare-metal stents: evidence from a comprehensive network meta-analysis. *Lancet.* 2012;379:1393-402.

3. Otsuka F, Cheng Q, Yahagi K, Acampado E, Sheehy A, Yazdani SK, Sakakura K, Euller K, Perkins LE, Kolodgie FD, Virmani R, Joner M. Acute Thrombogenicity of a Durable Polymer Everolimus-Eluting Stent Relative to Contemporary Drug-Eluting Stents With Biodegradable Polymer Coatings Assessed Ex Vivo in a Swine Shunt Model. *JACC Cardiovasc Interv.* 2015;8:1248-60.

4. Kolandaivelu K, Swaminathan R, Gibson WJ, Kolachalama VB, Nguyen-Ehrenreich KL, Giddings VL, Coleman L, Wong GK, Edelman ER. Stent thrombogenicity early in high-risk interventional settings is driven by stent design and deployment and protected by polymer-drug coatings. *Circulation.* 2011;123:1400-9.

5. von Birgelen C, Kok MM, van der Heijden LC, Danse PW, Schotborgh CE, Scholte M, Gin RMTJ, Somi S, van Houwelingen KG, Stoel MG, de Man FHAF, Louwerenburg JHW, Hartmann M, Zocca P, Linssen GCM, van der Palen J, Doggen CJM, Lowik MM. Very thin strut biodegradable polymer everolimus-eluting and sirolimus-eluting stents versus durable polymer zotarolimus-eluting stents in allcomers with coronary artery disease (BIO-RESORT): a three-arm, randomised, non-inferiority trial. *Lancet.* 2016;388:2607-17.

6. Saito S, Valdes-Chavarri M, Richardt G, Moreno R, Iniguez Romo A, Barbato E, Carrie D, Ando K, Merkely B, Kornowski R, Eltchaninoff H, James S, Wijns W; CENTURY II Investigators. A randomized, prospective, intercontinental evaluation of a bioresorbable polymer sirolimus-eluting coronary stent system: the CENTURY II (Clinical Evaluation of New Terumo Drug-Eluting Coronary Stent System in the Treatment of Patients with Coronary Artery Disease) trial. *Eur Heart J.* 2014;35:2021-31.

7. Costa RA, Abizaid A, Mehran R, Schofer J, Schuler GC, Hauptmann KE, Magalhaes MA, Parise H, Grube E; BioFreedom FIM Clinical Trial Investigators. Polymer-Free Biolimus A9-Coated Stents in the Treatment of De Novo Coronary Lesions: 4- and 12-Month Angiographic Follow-Up and Final 5-Year Clinical Outcomes of the Prospective, Multicenter BioFreedom FIM Clinical Trial. *JACC Cardiovasc Interv.* 2016;9:51-64.

8. Joner M, Finn AV, Farb A, Mont EK, Kolodgie FD, Ladich E, Kutys R, Skorija K, Gold HK, Virmani R. Pathology of drug-eluting stents in humans: delayed healing and late thrombotic risk. *J Am Coll Cardiol.* 2006;48:193-202.

9. Virmani R, Guagliumi G, Farb A, Musumeci G, Grieco N, Motta T, Mihalcsik L, Tespili M, Valsecchi O, Kolodgie FD. Localized hypersensitivity and late coronary thrombosis secondary to a sirolimus-eluting stent: should we be cautious? *Circulation.* 2004;109:701-5.

10. Nakazawa G, Otsuka F, Nakano M, Vorpahl M, Yazdani SK, Ladich E, Kolodgie FD, Finn AV, Virmani R. The pathology of neoatherosclerosis in human coronary implants bare-metal and drug-eluting stents. *J Am Coll Cardiol.* 2011;57:1314-22.

11. Koppara T, Cheng Q, Yahagi K, Mori H, Sanchez OD, Feygin J, Wittchow E, Kolodgie FD, Virmani R, Joner M. Thrombogenicity and early vascular healing response in metallic biodegradable polymer-based and fully bioabsorbable drug-eluting stents. *Circ Cardiovasc Interv.* 2015;8:002427.

12. Dunnett CW. A multiple comparison procedure for comparing several treatments with a control. *J Am Stat Assoc.* 1955;50:1096-121.

13. Szott LM, Irvin CA, Trollsas M, Hossainy S, Ratner BD. Blood compatibility assessment of polymers used in drug eluting stent coatings. *Biointerphases*. 2016;11:029806.

14. Mori H, Otsuka F, Gupta A, Jinnouchi H, Torii S, Harari E, Virmani R, Finn AV. Revisiting the role of durable polymers in cardiovascular devices. *Expert Rev Cardiovasc Ther.* 2017;15:835-46.

15. Garfinkle AM, Hoffman AS, Ratner BD, Reynolds LO, Hanson SR. Effects of a tetrafluoroethylene glow discharge on patency of small diameter dacron vascular grafts. *Trans Am Soc Artif Intern Organs.* 1984;30:432-9.

16. Kiaei D, Hoffman AS, Horbett TA. Tight binding of albumin to glow discharge treated polymers. *J Biomater Sci Polym Ed.* 1992;4:35-44.

17. Chinn JA, Sauter JA, Phillips RE Jr, Kao WJ, Anderson JM, Hanson SR, Ashton TR. Blood and tissue compatibility of modified polyester: thrombosis, inflammation, and healing. *J Biomed Mater Res.* 1998;39:130-40.

18. Petersen RJ, Rozelle LT. Ethylcellulose perfluorobutyrate: a highly non-thrombogenic fluoropolymer for gas exchange membranes. *Trans Am Soc Artif Intern Organs.* 1975;21:242-8.

19. Rogers C, Edelman ER. Endovascular stent design dictates experimental restenosis and thrombosis. *Circulation.* 1995;91:2995-3001.

20. Hasebe T, Yohena S, Kamijo A, Okazaki Y, Hotta A, Takahashi K, Suzuki T. Fluorine doping into diamond-like carbon coatings inhibits protein adsorption and platelet activation. *J Biomed Mater Res A.* 2007;83:1192-9.

21. Wertz CF, Santore MM. Effect of surface hydrophobicity on adsorption and relaxation kinetics of albumin and fibrinogen: Single-species and competitive behavior. *Langmuir.* 2001;17:3006-16.

22. Price MJ, Shlofmitz RA, Spriggs DJ, Haldis TA, Myers P, Popma Almonacid A, Maehara A, Dauler M, Peng Y, Mehran R. Safety and efficacy of the next generation Resolute Onyx zotarolimus-eluting stent: Primary outcome of the RESOLUTE ONYX core trial. *Catheter Cardiovasc Interv.* 2018;92:253-9.

23. Torii S, Nakazawa G, Ijichi T, Yoshikawa A, Ohno Y, Ikari Y. Comparison of the endothelial coverage in everolimus and zotarolimus-eluting stents in normal, atherosclerotic, and bifurcation rabbit iliac arteries. *Cardiovasc Interv Ther.* 2018;33:55-61.

24. Mori H, Atmakuri DR, Torii S, Braumann R, Smith S, Jinnouchi H, Gupta A, Harari E, Shkullaku M, Kutys R, Fowler D, Romero M, Virmani R, Finn AV. Very Late Pathological Responses to Cobalt-Chromium Everolimus-Eluting, Stainless Steel Sirolimus-Eluting, and Cobalt-Chromium Bare Metal Stents in Humans. *J Am Heart Assoc.* 2017 Nov 17;6(11).

25. Yazdani SK, Sheehy A, Pacetti S, Rittlemeyer B, Kolodgie FD, Virmani R. Stent Coating Integrity of Durable and Biodegradable Coated Drug Eluting Stents. *J Interv Cardiol.* 2016;29:483-90.

26. Basalus MW, Joner M, von Birgelen C, Byrne RA. Polymer coatings on drug-eluting stents: Samson's hair and Achilles' heel? *EuroIntervention.* 2013;9:302-5.

27. Tada N, Virmani R, Grant G, Bartlett L, Black A, Clavijo C, Christians U, Betts R, Savage D, Su SH, Shulze J, Kar S. Polymer-free biolimus a9-coated stent demonstrates more sustained intimal inhibition, improved healing, and reduced inflammation compared with a polymer-coated sirolimus-eluting cypher stent in a porcine model. *Circ Cardiovasc Interv.* 2010;3:174-83.

28. Chaabane C, Otsuka F, Virmani R, Bochaton-Piallat ML. Biological responses in stented arteries. *Cardiovasc Res.* 2013;99:353-63.

Supplementary data

Supplementary Appendix 1. Methods.

Supplementary Table 1A. Summary of the mean values from all animal blood coagulation (PT, PPT), platelet quantification (platelet counts, platelet estimates [EST]), activated platelet factor (PF4) as assessed by ELISA and activated clotting time (ACT), flow and shear rate in a swine acute shunt model.

Supplementary Table 1B. Second shunt experiment (FP-EES vs. BP-SES vs. BMS).

Supplementary Table 1C. Third shunt experiment (FP-EES vs. PF-BCS vs. BMS).

Supplementary Table 2A. Shunt matrix, first shunt experiment (FP-only vs. BMS).

Supplementary Table 2B. Shunt matrix, second shunt experiment (FP-EES vs. BP-SES vs. BMS).

Supplementary Table 2C. Shunt matrix, third shunt experiment (FP-EES vs. PF-BCS vs. BMS).

Supplementary Table 3. Estimated means with 95% confidence interval of percent fluorescence positive area by confocal microscopy (CM), platelet thrombus area by scanning electron microscopy (SEM), number of CD14 (monocytes) positive cells by CM, and number of PM-1 (neutrophils) positive cells by CM in a swine acute shunt model.

Supplementary Figure 1. Overview of stent profiles used in the current study.

The supplementary data are published online at: http://www.pcronline.com/eurointervention/149th_issue/289

Supplementary data

Supplementary Appendix 1. Methods.

Fabricating custom-made fluoropolymer-coated BMS (FP-only)

FP-only stents were fabricated in a manner as close as possible to the commercial XIENCE device. The mass of poly(vinylidene fluoride-co-hexafluoropropylene) [PVDF-HFP] coated on the FP-only stents was the same as the mass of PVDF-HFP found on this size of XIENCE Alpine™ stents (Abbott Vascular, Santa Clara, CA, USA). Inspection of the FP-only coatings by optical microscopy confirmed them to be of good quality. The catheters were taken from XIENCE Alpine™ production. The crimping process was done in the developmental clean room and yielded stent retention adequate to reliably deploy the FP-only stents in the tubing of the ex vivo model. The same terminal sterilisation process by ETO was used as for XIENCE Alpine™ commercial production.

Swine ex vivo arteriovenous shunt model

The study protocol was reviewed and approved by the Institutional Animal Care and Use Committee and met the ARRIVE guidelines. For each procedure, pigs were anaesthetised with ketamine/xylazine, intubated and maintained under general anaesthesia with isofluorane. A swine *ex vivo* carotid to jugular arteriovenous swine shunt model was established to study the extent of platelet adherence, thrombus formation, and acute inflammation as previously described. Three separate shunt studies were performed. In the first shunt study, custom-made fluoropolymer-only coated MULTI-LINK 8 BMS (Abbott Vascular, Santa Clara, CA, USA) without everolimus (FP-

only [n=8]) and MULTI-LINK 8 BMS (no polymer [n=7]) were compared. In the second shunt study, XIENCE Alpine™ (Abbott Vascular) EES with durable fluoropolymer (FP-EES [n=8]), Ultimaster® (Terumo Corp., Tokyo, Japan) abluminally coated biodegradable polymer sirolimus-eluting stent (BP-SES [n=8]), and MULTI-LINK VISION BMS (Abbott Vascular) (n=8) were compared. In the third shunt study, FP-EES (n=6), polymer-free Biolimus A9-coated stent (PF-BCS [n=6]) (BioFreedom™; Biosensors International, Singapore), and MULTI-LINK VISION BMS (n=6) were compared. Each shunt circuit had three stents and each animal had two shunt experiments with the exception of one animal which achieved only the first shunt experiment because of deterioration of its general condition that caused an unexpected platelet/inflammatory reaction to the Sylgard tubing during the second shunt experiment and therefore the second shunt experiment was not included in the analysis. In summary, a total of 57 stents were deployed in 19 shunts from 10 swine for the assessment of acute thrombogenicity **(Supplementary Table 2)**.

For each shunt run, three consecutive stents were deployed at nominal pressure in Sylgard mock vascular phantoms. The Sylgard conduits (ID 2.70 mm × 11 cm length) were fabricated using 316L stainless steel tubing and commercial silicone elastomer kit (Sylgard®-184; Dow Corning). Before deploying stents, the tubing was mounted in a fixed apparatus. The conduit was then filled with autologous serum and stents were expanded to 3.0 mm diameter at nominal pressure. The extent of platelet aggregation to struts was studied after exposure to circulating blood for one hour through an established arteriovenous carotid to jugular shunt.

Target blood activated clotting times (ACT) between 150 s and 190 s were achieved with intravenous heparin (100 IU/kg) dosing without antiplatelet agents such as clopidogrel or aspirin as the current study was specifically designed to examine inherent platelet-mediated thrombus formation induced by stents of differential design. Before establishing blood flow through the circuit, stents were primed with autologous platelet-poor plasma. During experiments, stented tubing was maintained in a 37°C water bath and flow rates were monitored continuously using an ultrasonic transducer (Transonic, Ithaca, NY, USA). At the conclusion of each run, stents were gravity perfused with Ringer's Lactate, fixed in 10% neutral buffered formalin and bisected longitudinally.

Assessment of platelet aggregation and inflammation

Sample fixation

After 60 minutes of continuous blood flow, the circuit was interrupted using a clamp and the Tygon tubing from the main Sylgard body (shunt) was disconnected. The stents were then gravity perfused with 250 mL Ringer's Lactate solution followed by 10% neutral buffered formalin. The most proximal end of the shunt (arterial side) was cut at an angle for orientation and the stents were then immersion-fixed in formalin for 20 minutes at room temperature, rinsed in PBS, and kept in 15% sucrose at 4°C until immunolabelling for platelets and inflammatory cells.

Confocal microscopy

After fixation, the stents were photographed and then carefully removed from the Sylgard tubing. Each stent was bisected longitudinally to expose the luminal surface. Stent halves were incubated

overnight in 4°C in an antibody cocktail directed against specific platelet markers: platelet cocktail of CD61, as a marker of platelet aggregation (Immunotech, IM0540, dilution 1:100; Beckman Coulter, CA, USA) and CD42b, as a marker of platelet adhesion (Santa Cruz, sc-7070, dilution 1:40) to capture both originating and propagated platelet thrombus. Each half was processed for immunostaining using inflammatory marker for neutrophils (PM-1; BMA Biological, Littleton, CO, USA; dilution 1:800) or monocytes (CD14; Novus Biological, Littleton, CO, USA; dilution 1:40). Positive staining was visualised using a secondary antibody conjugated to an Alexa Fluor® 488 fluorophore. After immunostaining, nuclei were counterstained with DAPI and stents were mounted *en face* on glass slides and coverslipped in aqueous mounting media. The entire stent surface was scanned using predetermined fixed parameters incorporating a tile feature with Z stack imaging (Zeiss, LSM 700, Zen 2011 software; Zeiss, Oberkochen, Germany). The positive area of platelet staining was analysed by proprietary software (Zen image analysis tool) within the entire bisected segment of the stented artery, which was maintained for all examined samples (40 mm^2) and reported as absolute positive area (mm^2) of the device and percentage of positive area which was calculated by dividing the absolute positive area by the entire bisected segment of the stented artery.

Scanning electron microscopy (SEM)

After confocal microscopy, stent halves were processed for SEM. Specimens were rinsed in 0.1M sodium phosphate buffer and post-fixed in 1% osmium tetroxide for approximately 30 minutes. The samples were then dehydrated in a graded series of ethanol, critically point dried, and sputter-coated with gold. Digital images were acquired using a Hitachi Model 3600N. Low-power (×15

magnification) images of the entire luminal surface were collected to assess the extent of thrombus attached to the strut surfaces. Stitched low-power montage images of the entire luminal surface were then assembled into a single image. Higher-power photographs of regions of interest were also taken at incremental magnifications of (×50, ×200, ×600, and ×2000). The percentage of thrombus coverage was estimated visually for each row of struts corresponding to a ring.

Quantification of inflammatory cells

Images for quantification of inflammatory cells were acquired at every other strut using a 20x long working distance objective (Plan-Neofluar 20x/0.50, WD=2.0 mm; Zeiss) in regions relatively free of platelet thrombus. The number of inflammatory cells was manually counted and expressed as cell density (cells/mm^2) relative to the strut surface area.

Blood coagulation and platelet function

Blood was serially drawn for coagulation and platelet function profiles pre-shunt (baseline) and after each experimental run to confirm the absence of coagulation and platelet function abnormalities. Indices of coagulation, platelet number and function included platelet count, prothrombin time (PT), partial thromboplastin time (PPT). In addition, pig platelet factor 4 (PF4) release was also assessed in collected plasma using a commercial ELISA kit (Cat No. ab156530, Abcam, Cambridge, MA, USA; sensitivity=0.1 ng/ml) according to the manufacturer's instructions.

Supplementary Figure 1. Overview of stent profiles used in the current study.

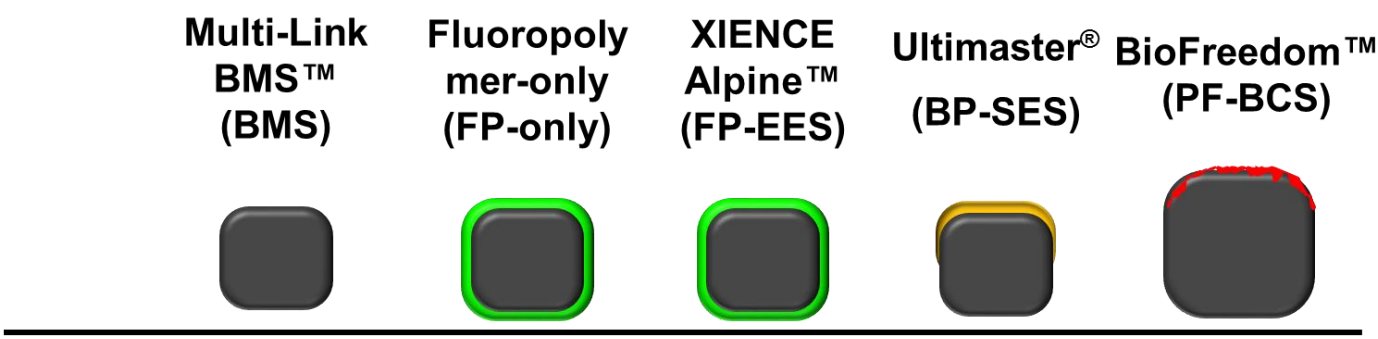

Platform	MULTI-LINK 8	MULTI-LINK 8	MULTI-LINK 8	Kaname	Juno
Material	CoCr	CoCr	CoCr	CoCr	Stainless Steel
Strut thickness	81 μm	81 μm	81 μm	80 μm	112 μm
Drug type	N/A	N/A	Everolimus	Sirolimus	BiolimusA9™
Drug dose	N/A	N/A	100 μg/cm^2	3.9 μg/mm	15.6 μg/mm
Materials of the polymer	N/A	PBMA/PVDF-HFP	PBMA/PVDF-HFP	Poly (DL-lactide-co-caprolactone)	No polymer
Coating type	N/A	Circumferential	Circumferential	Abluminal	Micro-structured Abluminal
Coating thickness	N/A	7-8 μm / side	7-8 μm / side	14 μm	N/A

Supplementary Table 1. Summary of the mean values from all animal blood coagulation (PT, PPT), platelet quantification (platelet counts, platelet estimates [EST]), activated platelet factor (PF4) as assessed by ELISA and activated clotting time (ACT), flow and shear rate in a swine acute shunt model.

Supplementary Table 1A. 1st shunt experiment (FP-only vs. BMS).

Test	Mean (Min - Max)			Fold change (%)		
	Baseline	After 1st shunt	After 2nd shunt	1st shunt vs. baseline	2nd shunt vs. baseline	2nd shunt vs. 1st shunt
Prothrombin time (seconds)	8.73 (8.1 – 9.5)	9.67 (8.9 – 10.2)	10.14 (8.6 – 11.4)	1.11	1.16	1.05
PPT (seconds)	10.8 (10.4 – 11.3)	45.9 (37.4 – 60.5)	54.9 (35.8 – 68.8)	4.25	5.08	1.20
Platelet count (x1000/μL)	155.3 (105 - 251)	187.3 (121 - 309)	170 (102 - 265)	1.21	1.09	0.91
Platelet EST	Adequate	Adequate	Adequate	N/A	N/A	N/A
Plasma PF4 assay	Below quantifiable value	Below quantifiable value	Below quantifiable value	N/A	N/A	N/A
ACT (seconds)	99.2 (94 – 105)	164.1 (148 – 182)	162.9 (144 – 174)	1.7	1.6	1.0
Flow rate (ml/minute)	N/A	139.0 (68-175)	158.8 (134-189)	N/A	N/A	N/A
Shear rate (Pa)	N/A	4.3 (2.1-5.4)	4.9 (4.1-5.8)	N/A	N/A	N/A

Platelet EST is considered to be adequate when the platelet count was estimated to be within the reference interval for swine.

PPT: partial thromboplastin time

Supplementary Table 1B. 2nd shunt experiment (FP-EES vs. BP-SES vs. BMS).

Test	Mean (Min - Max)			Fold change (%)		
	Baseline	After 1st shunt	After 2nd shunt	1st shunt vs. baseline	2nd shunt vs. baseline	2nd shunt vs. 1st shunt
Prothrombin time (seconds)	8.89 (8.1 – 9.7)	10.12 (8.9 – 10.8)	10.0 (8.8 – 10.7)	1.14	1.12	0.99
PPT (seconds)	11.52 (10.4 – 13.5)	40.9 (29.9 – 55.1)	47.88 (37.9 – 57.3)	3.55	4.16	1.17
Platelet count (x1000/μL)	311 (251 - 424)	279 (174 - 407)	271 (216 - 408)	0.90	0.87	0.97
Platelet EST	Adequate	Adequate	Adequate	N/A	N/A	N/A
Plasma PF4 assay	Below quantifiable value	Below quantifiable value	Below quantifiable value	N/A	N/A	N/A
ACT (seconds)	95.1 (87 – 104)	178.2 (158 – 214)	190.8 (150 – 255)	1.9	2.0	1.1
Flow rate (ml/minute)	N/A	120.4 (46.4-174)	136.8 (58-171)	N/A	N/A	N/A
Shear rate (Pa)	N/A	3.7 (1.4-5.3)	4.2 (1.8-5.2)	N/A	N/A	N/A

Platelet EST is considered to be adequate when the platelet count was estimated to be within the reference interval for swine.

PPT: partial thromboplastin time

Supplementary Table 1C. 3rd shunt experiment (FP-EES vs. PF-BCS vs. BMS).

Test	Mean (Min - Max)			Fold change (%)		
	Baseline	After 1st shunt	After 2nd shunt	1st shunt vs. baseline	2nd shunt vs. baseline	2nd shunt vs. 1st shunt
Prothrombin time (seconds)	9.3 (8.6 – 9.7)	10.87 (10.8 – 10.9)	11.33 (10.8 – 12)	1.17	1.22	1.04
PPT (seconds)	10.87 (9.3 – 12)	100 (33.6 – 100)	100 (73.1 – 100)	9.2	9.2	1.0
Platelet count (x1000/μL)	313.0 (186 – 454)	286.3 (224 – 360)	286.7 (232 – 385)	0.91	0.92	1.0
Platelet EST	Adequate	Adequate	Adequate	N/A	N/A	N/A
Plasma PF4 assay	Below quantifiable value	Below quantifiable value	Below quantifiable value	N/A	N/A	N/A
ACT (seconds)	100.2 (99.5 – 101)	174.8 (142 – 229)	170.9 (137 – 208)	1.7	1.7	1.0
Flow rate (ml/minute)	N/A	109.9 (40-144)	110.2 (65-156)	N/A	N/A	N/A
Shear rate (Pa)	N/A	3.4 (1.2-4.4)	3.4 (2.0-4.8)	N/A	N/A	N/A

Platelet EST is considered to be adequate when the platelet count was estimated to be within the reference interval for swine.

PPT: partial thromboplastin time

Supplementary Table 2. Assessment of acute thrombogenicity.

Supplementary Table 2A. Shunt matrix, 1st shunt experiment (FP-only vs. BMS).

1st shunt	FP-only vs. BMS			
Animal number	**Shunt**			**Shunt run**
	Number	**Position**	**Stents**	
1	1	Proximal	**BMS**	1 hr
		Middle	**FP-only**	
		Distal	**BMS**	
	2	Proximal	**FP-only**	1 hr
		Middle	**BMS**	
		Distal	**FP-only**	
2	3	Proximal	**BMS**	1 hr
		Middle	**FP-only**	
		Distal	**BMS**	
	4	Proximal	**FP-only**	1 hr
		Middle	**BMS**	
		Distal	**FP-only**	
3	5	Proximal	**FP-only**	52 min
		Middle	**BMS**	
		Distal	**FP-only**	

Supplementary Table 2B. Shunt matrix, 2nd shunt experiment (FP-EES vs. BP-SES vs. BMS).

2nd shunt	FP-EES vs. BP-SES vs. BMS			
Animal number	**Shunt**			**Shunt run**
	Number	**Position**	**Stents**	
3	6	Proximal Middle Distal	**BMS** **FP-EES** **BP-SES**	52 min
4	7	Proximal Middle Distal	**BMS** **FP-EES** **BP-SES**	1 hr
	not included			
5	8	Proximal Middle Distal	**BMS** **FP-EES** **BP-SES**	1 hr
	9	Proximal Middle Distal	**FP-EES** **BP-SES** **BMS**	1 hr
6	10	Proximal Middle Distal	**BP-SES** **BMS** **FP-EES**	1 hr
	11	Proximal Middle Distal	**BMS** **FP-EES** **BP-SES**	1 hr
7	12	Proximal Middle Distal	**FP-EES** **BP-SES** **BMS**	55 min
	13	Proximal Middle Distal	**BMS** **FP-EES** **BP-SES**	1 hr

Supplementary Table 2C. Shunt matrix, 3rd shunt experiment (FP-EES vs. PF-BCS vs. BMS).

3rd shunt	FP-EES vs. PF-BCS vs. BMS			
	Shunt			Shunt run
Animal number	Number	Position	Stents	
8	14	Proximal	**FP-EES**	55 min
		Middle	**PF-BCCS**	
		Distal	**BMS**	
	15	Proximal	**PF-BCCS**	59 min
		Middle	**BMS**	
		Distal	**FP-EES**	
9	16	Proximal	**BMS**	1 hr
		Middle	**FP-EES**	
		Distal	**PF-BCS**	
	17	Proximal	**FP-EES**	1 hr
		Middle	**PF-BCS**	
		Distal	**BMS**	
10	18	Proximal	**PF-BCS**	1 hr
		Middle	**BMS**	
		Distal	**FP-EES**	
	19	Proximal	**BMS**	1 hr
		Middle	**FP-EES**	
		Distal	**PF-BCCS**	

Supplementary Table 3. Estimated means with 95% confidence interval of percent fluorescence positive area by confocal microscopy (CM), platelet thrombus area by scanning electron microscopy (SEM), number of CD14 (monocytes) positive cells by cm, and number of PM-1 (neutrophils) positive cells by CM in a swine acute shunt model.

Shunt experiment 2	BMS 1		BMS 2		BMS 3		BMS 1 vs. BMS 2 *p*-value	BMS 1 vs. BMS 3 *p*-value	BMS 2 vs. BMS 3 *p*-value
CD42b/CD61 positive area, % by CM	13.1	(4.3-39.7)	22.6	(9.2-55.5)	19.7	(6.2-63.1)	0.4	0.6	0.8
CD42b/CD61 positive area, % by SEM	23.2	(8.6-62.1)	24.6	(10.9-55.5)	25.3	(9.0-71.4)	0.9	0.9	0.97
CD14 positive cells, cell number/mm^2	381.1	(207.9-698.7)	387.3	(235.8-636.1)	533.8	(298.5-954.4)	0.97	0.4	0.4
PM-1 positive cells, cell number/mm^2	213.6	(148.7-306.8)	283.6	(212.6-378.4)	287.7	(205.6-402.5)	0.2	0.2	0.95

Values are expressed as estimated mean with 95% confidence interval.